Validation of Two-Layer Model for Underexpanded Hydrogen Jets

Xuefang Li[a], Bikram Roy Chowdhury[b], Qian He[a], David M Christopher[c,*], Ethan S Hecht[b,*]

[a]Institute of Thermal Science and Technology, Shandong University, Jinan 250061, China

[b]Combustion Research Facility, Sandia National laboratories, Livermore, CA 94550, USA

[c]Key Laboratory of Thermal Science and Power Engineering of Ministry of Education, Tsinghua University, Beijing 100084, China

[*]Corresponding authors: dmc@tsinghua.edu.cn, ehect@sandia.gov.

Abstract: Previous studies have shown that the two-layer model more accurately predicts hydrogen dispersion than any of the conventional notional nozzle models without significantly increasing the computational expense. However, the model was lacking validation in some aspects, specifically the ability to predict both the concentration and velocity distributions. In the present study, particle imaging velocimetry (PIV) was used to measure the velocity field of an underexpanded hydrogen jet released at 10 bar from a 1.5 mm diameter orifice. The two-layer model was used to calculate the inlet conditions for a subsequent two-dimensional axisymmetric CFD model to simulate the hydrogen jet downstream of the Mach disk. The predicted velocity spreading and centerline decay rates agreed well with the measurements. The predicted concentration distribution was consistent with data from a previous planar Rayleigh scattering measurement. The jet spreading was also simulated using several widely used notional nozzle models combined with the integral plume model for comparison. The results show that the velocity and concentration distributions are both better predicted by the two-layer model than the notional nozzle models. Though more validation studies are needed to improve confidence in the model and increase the range of validity, the present work indicates that the two-layer model is a promising tool for fast, accurate predictions of the flow fields of underexpanded hydrogen jets.

Keywords: two-layer model, PIV, hydrogen safety, underexpanded jets

1 Introduction

Hydrogen is an energy carrier that enables a path to reduce and even eliminate fossil fuel use for transportation and stationary energy applications. Hydrogen can be generated from sustainable, carbon-free energy sources, stored, transported, and then utilized at a different time and/or place to generate power or motility. A major commercial application of hydrogen is fuel cell vehicles that have favorable short refueling times of only a few minutes and ranges that are similar to those of fossil-fueled vehicles [1]. All of the consumer fuel cell vehicles on the road today, including the Toyota Mirai, Honda Clarity Fuel Cell, and Hundai Nexo, have hydrogen stored at high pressure (700 bar) to have the fuel capacity for a similar range as fossil-fueled vehicles in a reasonably compact storage volume. Simulations of unintended releases from high pressure vessels and plumbing can be used to ensure the safety of vehicles and refueling infrastructure.

Birch et al. [2] measured and demonstrated that the downstream concentration field of choked jets (above the critical pressure) appears to be equivalent to a subsonic turbulent free jet, if it is scaled by a larger source diameter than the actual diameter of the release. Birch and coworkers followed up this work by measuring the centerline velocity of supersonic air jets and improved upon their pseudo-source calculations [3]. As discussed in more detail later, several notional nozzle models with different assumptions have been developed to calculate this pseudo-source for choked jets [4-7]. However, these models have limited experimental validation often with validation of only one aspect (e.g. either concentration or velocity) of the predictions.

Computational fluid dynamics (CFD) models often span a range of length and time scales. In the case of high pressure hydrogen releases, the near nozzle-region contains complex shock structures with regions of immense property gradients around the shocks. Recently, adaptive mesh refinement techniques have made (nearly) direct numerical simulations of high pressure hydrogen jets possible on a supercomputer [8]. The more common approach is to use large eddy simulation (LES) or Reynolds averaged Navier-Stokes (RANS) techniques to limit the length or time resolution necessary for the simulations. To further simplify the problem and reduce the computational resources needed, notional nozzle models can be used to generate the boundary conditions for the CFD simulation [9].

In this work, we present new measurements of the two-dimensional velocity field of an unignited

10 bar hydrogen jet. We use the same two-layer notional nozzle described by Li et al. [9] to generate boundary conditions for a RANS model. By comparing both the downstream velocity and concentration to experimental measurements, we ensure that this modeling approach accurately predicts the flow-fields. We show the accuracy of this computationally efficient method for simulating high-pressure hydrogen releases.

2 Experimental Methodology

The high pressure stagnation chamber capable of operating at pressure ratios up to 60:1 described by Ruggles and Ekoto [10] was used to study the hydrogen jet release. For this work, a hydrogen jet with a 10:1 pressure ratio (stagnation to ambient pressure) was investigated using a 1.5 mm diameter nozzle. Instantaneous velocity measurements were recorded using the Particle Image Velocimetry (PIV) technique. The PIV system consisted of a dual cavity 250 mJ/pulse Nd:YAG laser (Spectra Physics PIV-400), a frame straddling CCD camera (Imager Pro -X) and the DaVis 8.3 post-processing software. A laser sheet was created by expanding and focusing the beams using a cylindrical plano-concave (f = –500 mm) and spherical plano-convex (f = 1000 mm) lens pair. The laser sheet had a constant height of 20 mm along the region of interest and was aligned along the center plane of the nozzle. Sub-micron sized titanium dioxide particles were used to seed the flow. The time between laser pulses was adjusted to ensure that the particles in the flow traveled roughly one quarter of the interrogation window width. The PIV camera was equipped with a Nikon 50-mm focal length lens fitted with a 3.0 Neutral Density filter.

Ten areas above the nozzle exit were sampled, starting 80 mm downstream of the nozzle. The pressure chamber assembly was traversed downwards in 16 mm increments to obtain velocity measurements up to 240 mm downstream of the nozzle. At each position, 500 Mie scattering image pairs were acquired.

The LaVision DaVis 8.3 software was used for processing the Mie scattering images. Following background subtraction, a multi-pass cross correlation algorithm was used starting with an interrogation window size of 128 × 128 pixels and finally reducing to an interrogation window size of 16 × 16 pixels with 50% overlap. Ensemble averaged velocity profiles were computed from the instantaneous velocity measurements for each section. The mean velocity fields from each sectional interrogation region were then combined into a reconstruction of the complete velocity field. The

final vector field resolution was 1.24 × 1.24 mm.

3 Model descriptions

3.1 Integral model

The first-order jet model described by Winters and Houf [11,12] is based on the integral turbulent jet model [13]. The model has been incorporated into the Sandia developed HyRAM toolkit and can handle both cryogenic and high pressure flows. Briefly, the flow field of an underexpanded jet can be qualitatively divided into (potentially) four successive zones: (I) underexpanded flow, (II) initial entrainment and heating, (III) flow establishment, and (IV) established flow zone, as shown in Fig. 1.

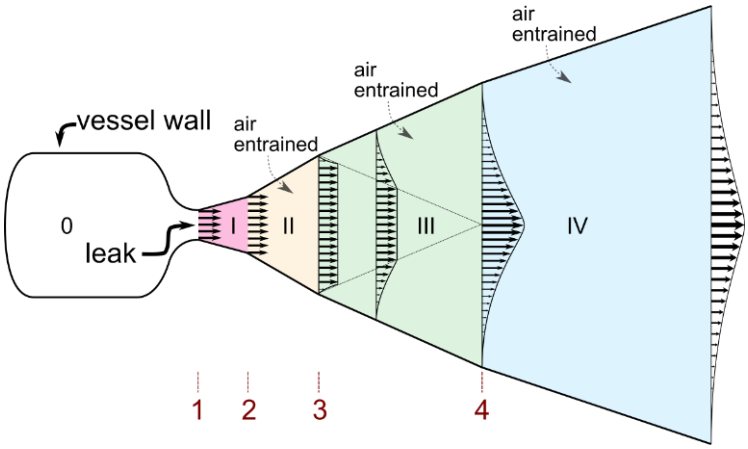

Fig. 1. Schematic of an underexpanded jet.

Zones I to III are relatively small compared with Zone IV which is the major part of the flow field. There is no Zone I for a subsonic jet since the flow has already expanded to the ambient pressure at the nozzle exit. In Zone II, if necessary such that the jet heats up to a point where the constituents of air no longer condense, the flow is assumed to be fully turbulent and quasi-steady. Therefore, a plug-flow model is used to model the flow which assumes that the radial velocity and jet scalar distributions are uniform and the gas pressure is equal to the ambient pressure. The flow transforms into a fully developed jet flow in Zone III. Zone IV is the fully developed flow region in which the jet velocity, density and hydrogen mass fractions are assumed to have Gaussian profiles in the radial direction as

$$V = V_{cl} \exp\left(-\frac{r^2}{B^2}\right), \tag{1}$$

$$\rho - \rho_\infty = (\rho_{cl} - \rho_\infty) \exp\left[-\frac{r^2}{(\lambda B)^2} \right], \tag{2}$$

$$\rho Y = \rho_{cl} Y_{cl} \exp\left[-\frac{r^2}{(\lambda B)^2} \right], \tag{3}$$

where V is the velocity, ρ is the density, Y is the hydrogen mass fraction, and r is the jet radial coordinate. The subscript "cl" denotes along the jet centerline and ∞ represents the atmospheric conditions. λ is the relative spreading ratio between the jet scalars such as density and mass fraction and the jet velocity. For more details of the model, the readers are referred to the literature [11, 13, 14].

3.2 Notional nozzle model

The underexpanded flow zone (Zone I) is needed for high pressure leaks because of the complex near field shock structures. This zone is often termed a notional nozzle model and provides effective boundary conditions for the integral model. The stagnation state is denoted by 0, the real nozzle exit is denoted by 1 and the effective nozzle exit is denoted by 2, as shown in Fig. 2.

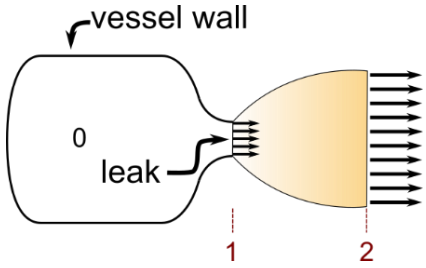

Fig. 2. Schematic of the notional nozzle model.

Several notional nozzle models have been developed by Birch et al. [3,13], Molkov et al. [15], Yuceil and Otugen [4], and Harstad and Bellan [5]. These all predict a notional nozzle size and flow velocity through the notional nozzle region with the two models by Birch et al. [2,3] assuming that the gas temperature at the notional nozzle is equal to the ambient temperature while Yuceil and Otugen [4] calculate the gas temperature at the notional nozzle. The model by Molkov et al. [15] assumes that the velocity after the notional nozzle exit is at the sonic speed and uses the Abel-Noble real gas properties. Harstad and Bellan [5] assume the pressure at the notional nozzle is equal to the ambient pressure and use the entropy production relationship.

3.3 Two-layer model

An underexpanded hydrogen gas jet contains three flow regions, i.e. the nearfield, the transition and the farfield zones. The jet nearfield contains a core flow region and a mixing layer. In the core flow region, the gas flow expands to supersonic speeds with the highest Mach number just upstream of the Mach disk. The hydrogen gas then passes through the Mach disk where the gas pressure suddenly increases to atmospheric pressure, the temperature approaches ambient temperature and the velocity decreases to a subsonic velocity. The rest of the hydrogen gas flows into the mixing layer with air entrained into the flow then bypassing the Mach disk at supersonic velocities. The two-layer model takes the flow partitioning phenomenon into account, as shown in Fig. 3, with the following assumptions:

(1) The radial distributions of the velocity and other flow parameters are uniform (plug flows) in each layer, i.e. the core flow and the mixing layer.

(2) The pressures in both layers approach atmospheric pressure.

(3) The flow expands isentropically from the jet exit to the Mach disk plane.

(4) The ideal gas equation can be used to calculate the air and hydrogen densities.

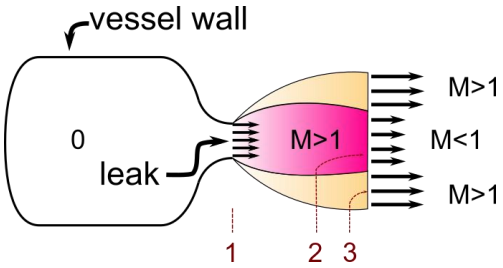

Fig. 3. Schematic of the two-layer model.

Then, the conservation equations from the nozzle exit to the Mach disk plane are:

$$\dot{m}_1 = \dot{m}_2 + Y_3 \rho_3 V_3 A_3 , \tag{4}$$

$$p_1 A_1 + \dot{m}_1 V_1 = p_{2b} A_1 + \dot{m}_2 V_{2b} + \rho_3 A_3 V_3^2 , \tag{5}$$

$$\dot{m}_1 \left(c_{p,\mathrm{H2}} T_1 + \frac{V_1^2}{2} \right) = \dot{m}_2 \left(c_{p,\mathrm{H2}} T_{2b} + \frac{V_{2b}^2}{2} \right) + \rho_3 A_3 V_3 \left[c_{p,3} T_3 + \frac{V_3^2}{2} - \left(1 - Y_3\right) c_{p,\mathrm{air}} T_\infty \right] . \tag{6}$$

In Eqs. (4) to (6), $\dot{m}$ is the mass flow rate, A denotes the area, T is the temperature, and c_p is the specific heat capacity. The subscripts denote the state points shown in Fig. 3, with "a" denoting upstream and "b" denoting downstream of the Mach disk.

The flow conditions at the nozzle exit (state 1) can be calculated using the choked flow equations assuming an isentropic expansion from the vessel. The necessary spatial parameters, such as the Mach disk location and diameter and the mixing layer thickness are obtained from the literature and previous experimental studies [16]:

$$z/d_1 = 0.67\sqrt{p_0/p_\infty},\ d_2/d_1 = 0.35\sqrt{p_0/p_\infty},\ b_3/d_1 = 0.30\sqrt{p_0/p_\infty} \tag{7}$$

where z is the Mach disk location, d_2 is the Mach disk diameter and b_3 is the mixing layer thickness. More details of the two-layer model were given earlier [9,14].

3.4 CFD model settings

The inlet conditions generated by the two-layer model were used to simulate the downstream jet in a two-dimensional axisymmetric domain, as shown in Fig. 4 which also specifies the boundary conditions.

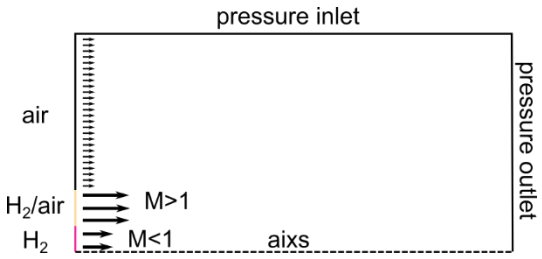

Fig. 4. Computational domain.

The model solved the steady state Reynolds-averaged Navier-Stokes (RANS) equations including the energy equation and the species transport equation with turbulent flow. The realizable k-ε model was used for the turbulence. A pressure based solver was used with the ideal gas equation of states to calculate the gas density. The flow equations were discretized by a second order upwind scheme and the SIMPLE scheme was used for the pressure-velocity coupling.

Three models were used with 28,000, 35,560, and 44,100 elements with all three meshes giving nearly the same results. The results reported here are for the mesh with 35,560 elements. All the calculations used Fluent 14 on a personal computer with the calculations taking only a few hours to finish in each case.

4 Results

4.1 Velocity

The measured mean velocity distribution is shown in Fig. 5.

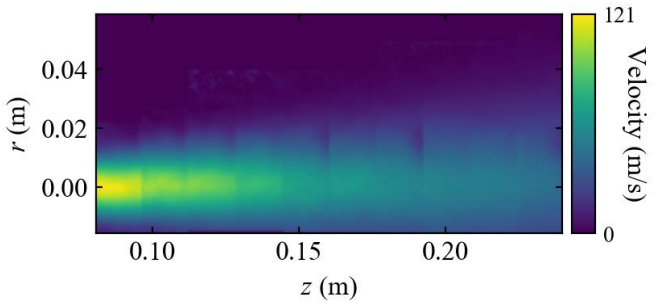

Fig. 5. Mean velocity field measured by PIV.

Four velocity contours predicted by the two-layer model are compared with the measured data in Fig. 6 with the measurements in the top half of the figure and the predictions in the bottom half. The two-layer model predictions agree reasonably well with the measured velocity field with the predictions slightly overestimating the downstream distance of the 65 and 95 m/s centerline velocity contours.

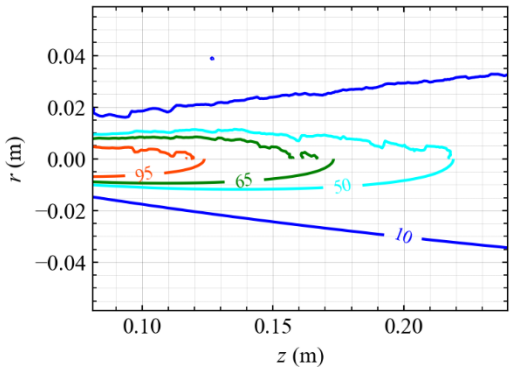

Fig. 6. Comparison of the predicted and measured velocity contours (m/s). The upper half (r>0) is the PIV data while the lower half (r<0) shows the predictions.

The measured mean velocity decay along the jet centerline is shown in Fig. 7 with the mean velocity normalized by the jet velocity at the nozzle exit, V_t, and the axial distance, z, normalized by the orifice radius, r_0. The velocity decays linearly with the axial distance from the nozzle exit, as has been often noted in former studies [4]. The calculated velocity decays using the notional nozzle models and the two-layer model are also shown in Fig. 7. The two-layer model gives the closest predictions to the experimental data, while most of the notional nozzle models significantly

underestimate the velocity decay rate except for the Hastard model which overpredicts the velocity decay rate.

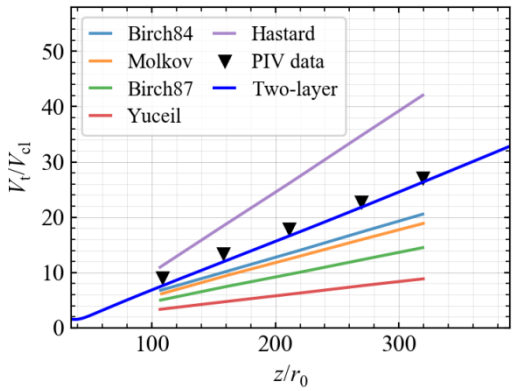

Fig. 7. Reciprocal mean velocities along the jet centerline.

The radial velocity distributions at different axial locations are shown in Fig. 8. In Fig. 8, the points represent the PIV data while the solid lines with the same color represent the calculated results using the two-layer model. The calculated radial velocity profiles agree with the measurements, with slight overpredictions of the centerline velocities at locations close to the nozzle as was seen in Fig. 7.

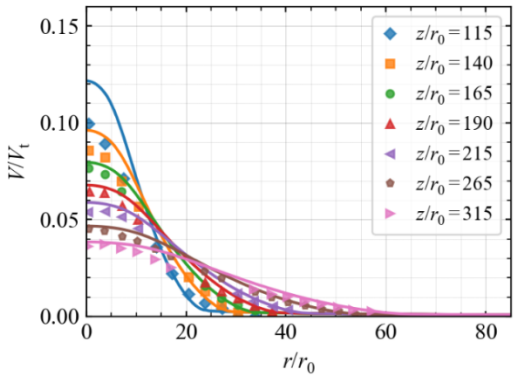

Fig. 8. Radial velocity profiles at various axial locations. The points are the PIV data while the solid lines are the predictions of the two-layer model.

The results shown in Fig. 7 and Fig. 8 indicate that the PIV measurements were in the fully developed zone. In other words, the radial velocity distributions have Gaussian profiles. Furthermore, all the data points collapse onto a single Gaussian curve because of the self-preservation characteristics with the radial coordinate being normalized by the axial distance, as shown in Fig. 9. The curve fit of all the data shown in Fig. 9 gives a coefficient of 78.1 related to the half width of the Gaussian profile, which is very close to the literature value of 76.8 [4].

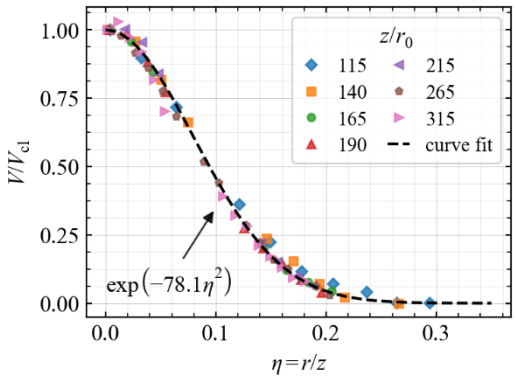

Fig. 9. Normalized radial profiles of the measured velocity field.

The nearfield velocity distribution predicted by the two-layer simulation is shown in Fig. 10. The velocities in the slip region are substantially larger than those coming out of the Mach disk. The flow partitioning characteristics of the two-layer model better simulate the jet downstream of the Mach disk than the notional nozzle models which only have a single plug flow with a uniform velocity profile at the notional nozzle. The partitioned velocity profile is also very helpful in simulating release scenarios which have obstacles in the vicinity of the leak orifice [17].

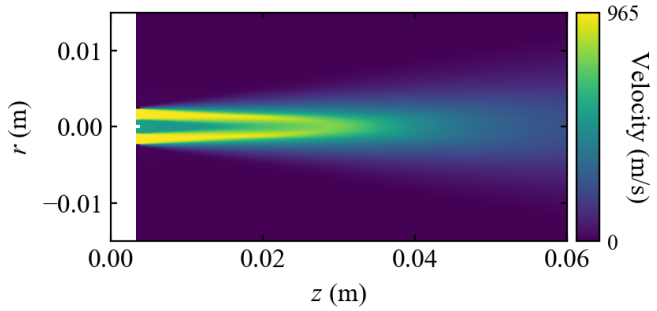

Fig. 10. Nearfield velocity distribution predicted by the two-layer model.

4.2 Concentration

Four predicted mean mole fraction contours are plotted in Fig. 11 (mole fractions of 0.3, 0.2, 0.1 and 0.04). The mole fraction of 0.04 corresponds to the lean flammability limit of a static hydrogen/air mixture. Fig. 11 shows that the two-layer model simulation also gives reasonable predictions of the jet concentration distributions.

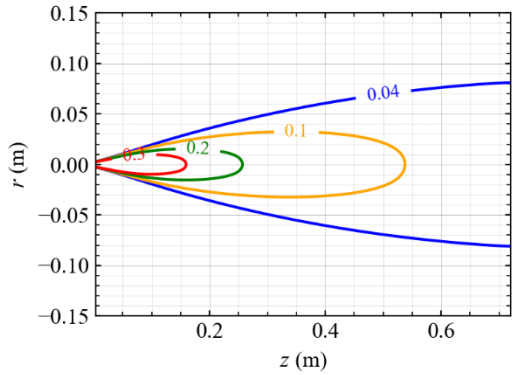

Fig. 11. Predicted hydrogen mole fraction contours.

Although there is no direct concentration data for comparison, the calculated hydrogen mass fraction decay is compared to previous planar laser Rayleigh scattering (PLRS) measurements by Ruggles and Ekoto [10] in Fig. 12. The notional nozzle predictions are also included for comparison. The two-layer, Birch87 and Yuceil models well predict the centerline mass fraction decay, with the other models underestimated the decay rate.

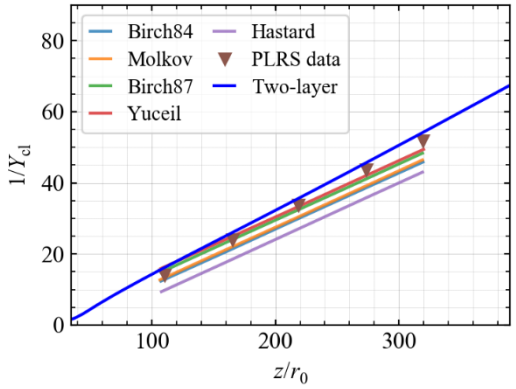

Fig. 12. Centerline mass fraction decay.

The calculated radial profiles of the normalized hydrogen mass fraction also collapse onto a Gaussian curve like the velocity profiles as shown in Fig. 13. A curve fit of all the normalized profiles gives a coefficient of 60.0 which is very close to the literature value of 59 for jets of different gases and test conditions [18]. The curve fit coefficients for the curve fits of the two-region model predictions in Fig. 9 and Fig. 13 can be related to give the relative spreading ratio between the mass fraction and velocity profiles, λ, calculated as:

$$\lambda = \sqrt{78.1/60.0} = 1.14 \tag{8}$$

which is very close to the widely used value of 1.16.

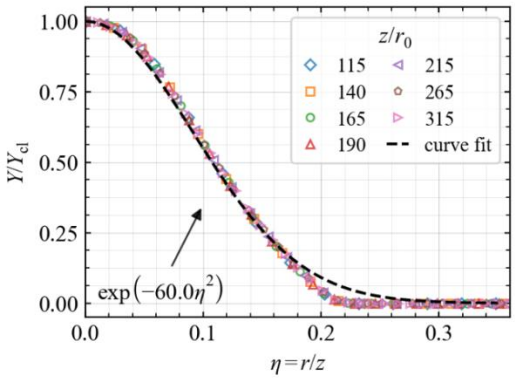

Fig. 13. Normalized radial profiles of the calculated mass fractions.

5 Conclusions and future work

In this study, the two-layer model was validated by comparing predicted velocity and concentration profiles to measured data for an underexpanded hydrogen jet released at 10 bar from a 1.5 mm diameter orifice. The velocity field was measured using a PIV system with the concentration data obtained from previous PLRS measurements by Ruggles and Ekoto [10]. Both measurements used the same hydrogen release system in the Combustion Research Facility at Sandia National Laboratories, which gives good consistency between the velocity and concentration measurements. Several notional nozzle models were also evaluated for comparison.

The results show that although most of the notional nozzle models reasonably predict the jet centerline mass fraction decay, none of them well predict the centerline velocity decay. However, the two-layer model accurately predicts both the measured velocity and concentration distributions. Although the two-layer model has to be combined with a CFD model for simulations (until a simplified model for a transition region to fully developed flow is developed), the computing expense has been significantly reduced compared with conventional full CFD simulations, which would require high resolution meshes in the shock region. Therefore, the two-layer model is a promising tool for fast, accurate predictions of the flow fields of underexpanded hydrogen jets, especially when the integral jet model cannot be used because of obstacles in the flow field.

Acknowledgements

This study was supported by the Shandong Provincial Natural Science Foundation, China (No. ZR2017BEE003), the National Natural Science Foundation of China (Nos. 51706125 and 51476091), the China Postdoctoral Science Foundation (No. 2017M612267), and the Fundamental

Research Funds of Shandong University. Sandia National Laboratories is a multi-mission laboratory managed and operated by National Technology and Engineering Solutions of Sandia, LLC., a wholly owned subsidiary of Honeywell International, Inc., for the U.S. Department of Energy's National Nuclear Security Administration under contract DE-NA0003525. This paper describes objective technical results and analysis. Any subjective views or opinions that might be expressed in the paper do not necessarily represent the views of the U.S. Department of Energy or the United States Government.

References

[1] Molkov V. Fundamentals of Hydrogen Safety Engineering. bookboon.com, 2012.

[2] Birch AD, Brown DR, Dodson MG, Swaffield F. The structure and concentration decay of high pressure jets of natural gas. COMBUST SCI TECHNOL. 1984; 36:249-61.

[3] Birch AD, Hughes DJ, Swaffield F. Velocity decay of high pressure jets. COMBUST SCI TECHNOL. 1987; 52:161-71.

[4] Yuceil KB, Otugen MV. Scaling parameters for underexpanded supersonic jets. PHYS FLUIDS. 2002; 14:4206-15.

[5] Harstad K, Bellan J. Global analysis and parametric dependencies for potential unintended hydrogen-fuel releases. COMBUST FLAME. 2006; 144:89-102.

[6] Schefer RW, Houf WG, Williams TC, Bourne B, Colton J. Characterization of high-pressure, underexpanded hydrogen-jet flames. INT J HYDROGEN ENERG. 2007; 32:2081-93.

[7] Molkov V, Saffers J. Hydrogen jet flames. INT J HYDROGEN ENERG. 2013; 38:8141-58.

[8] Tang X, Dzieminska E, Asahara M, Hayashi AK, Tsuboi N. Numerical investigation of a high pressure hydrogen jet of 82 MPa with adaptive mesh refinement: Concentration and velocity distributions. INT J HYDROGEN ENERG. 2018; 43:9094-109.

[9] Li X, Christopher DM, Hecht ES, Ekoto IW. Comparison of two-layer model for hydrogen and helium jets with notional nozzle model predictions and experimental data for pressures up to 35 MPa. INT J HYDROGEN ENERG. 2017; 42:7457-66.

[10] Ruggles AJ, Ekoto IW. Ignitability and Mixing of Underexpanded Hydrogen Jets. INT J HYDROGEN ENERG. 2012; 37:17549-60.

[11] Winters WS, Houf WG. Simulation of small-scale releases from liquid hydrogen storage systems. INT J HYDROGEN ENERG. 2011; 36:3913-21.

[12] Houf WG, Winters WS. Simulation of high-pressure liquid hydrogen releases. INT J HYDROGEN ENERG. 2013; 38:8092-9.

[13] Gebhart B, Hilder DS, Kelleher M. The Diffusion of Turbulent Buoyant Jets. Advances in heat transfer. 1984:1-57.

[14] Li X, Hecht ES, Christopher DM. Validation of a reduced-order jet model for subsonic and underexpanded hydrogen jets. INT J HYDROGEN ENERG. 2016; 41:1348-58.

[15] Molkov V, Makarov D, Bragin M. Physics and modelling of underexpanded jets and hydrogen dispersion in atmosphere. The 24th International Conference on Interaction of Intense Energy Fluxes with Matter, Elbrus, 2009.

[16] Hecht E, Li X, Ekoto IW. Validated equivalent source model for an underexpanded hydrogen jet. International Conference on Hydrogen Safety, Yokohama, Japan, 2015.
[17] Hu J, Christopher DM, Li X. Simplified partitioning model to simulate high pressure under-expanded jet flows impinging vertical obstacles. INT J HYDROGEN ENERG. 2018; 43:13649-58.
[18] Schefer R, Houf W, Williams T. Investigation of small-scale unintended releases of hydrogen: momentum-dominated regime. INT J HYDROGEN ENERG. 2008; 33:6373-84.